



In silico modelling of protein digestion: A case study on solid/liquid and blended meals

Andrea Rivera del Rio^a, Nikkie van der Wielen^b, Walter J.J. Gerrits^b, Remko M. Boom^a, Anja E. M. Janssen^{a,*}

^a Food Process Engineering, Wageningen University, 6700 AA Wageningen, the Netherlands

^b Animal Nutrition, Wageningen University, 6700 AH Wageningen, the Netherlands

ARTICLE INFO

Keywords:

In silico digestion
Physiologically based models
Compartmental models
Protein digestion
Gastric emptying
Antral grinding

ABSTRACT

We present a dynamic, semi-mechanistic, compartmental protein digestion model to study the kinetics of protein digestion. The digestive system is described as a series of eight compartments: one for the stomach, one for the duodenum, two for the jejunum and four for the ileum. The digestive processes are described by a set of zero or first order differential equations. The model considers ingestion of a meal, secretion of gastric and pancreatic juices, protein hydrolysis, grinding, transit and amino acid absorption. The model was used to simulate protein digestion of a meal composed of a solid and a liquid phase or one where both phases are blended into a homogeneous phase. Luminal volumes and pH of gastric and duodenal contents were estimated for both meals. Further, gastric emptying is described as a function of the energy density of the bolus, instead of the more common mass action approach.

1. Introduction

In the last decades, *in vitro* models have aided in the study of food digestion complementing *in vivo* studies (Lucas-González et al., 2018). *In silico* models have only recently gained some momentum but have the potential to aid and steer the whole field by identifying causality, gaps and inconsistencies in our understanding (Le Feunteun, Al-Razaz, et al., 2021; Le Feunteun et al., 2020). *In vitro* and *in silico* models are both simplified representations of the complex processes occurring during *in vivo* digestion. These models can integrate different stages of food digestion and shed more light on the underlying mechanisms. Le Feunteun, Verkempinck, et al. (2021) showcased the complementary value of *in silico* and *in vitro* dynamic models, regarding hydrolysis kinetics in particular.

The use of physiologically based models to describe food digestion borrows concepts from the field of pharmacokinetics, i.e. the study of the kinetics of absorption, distribution, metabolism and excretion of pharmaceutical compounds (Turfus et al., 2017). Physiological systems are described as a set of interconnected biological compartments, often anatomical parts of the organism under study. In animal nutrition works, compartmental models have been used to study digestion in pigs

(Bastianelli et al., 1996; Rivest et al., 2000; Strathe et al., 2008). Halas et al. (2018) gathered a comprehensive collection of feed intake, digestion kinetics, utilization and animal growth models. Meanwhile, Le Feunteun, Al-Razaz, et al. (2021) reviewed the models and tools currently available to study food digestion in humans and provided an outlook to the potential of the developing field. This review draws attention to the work of van Aken (2020), in which the digestion and absorption of all nutrients is simulated in a multicompartmental model that is able to predict hormonal responses, feedback mechanisms and interindividual variations. Mathematical models allow the replication of the dynamic nature of digestion, not only in terms of the flow within and throughout the gastrointestinal tract, but also the physicochemical properties of the food and its environment (van der Sman et al., 2020).

Provided that enough knowledge on the underlying mechanisms is available, it is also possible to incorporate feedback processes. *In silico* models can therefore aid in understanding and quantifying abstract events and processes occurring during the digestion of food. In this way, *in silico* models contribute to understanding and predicting nutrient absorption kinetics.

In this work, we developed a dynamic model of protein digestion, incorporating endogenous secretions, antral grinding, hydrolysis,

* Corresponding author.

E-mail addresses: andrea.riveradelrio@wur.nl (A. Rivera del Rio), nikkie.vanderwielen@wur.nl (N. van der Wielen), walter.gerrits@wur.nl (W.J.J. Gerrits), remko.boom@wur.nl (R.M. Boom), anja.janssen@wur.nl (A.E.M. Janssen).

<https://doi.org/10.1016/j.foodres.2022.111271>

Received 23 February 2022; Received in revised form 13 April 2022; Accepted 17 April 2022

Available online 20 April 2022

0963-9969/© 2022 The Authors. Published by Elsevier Ltd. This is an open access article under the CC BY-NC-ND license (<http://creativecommons.org/licenses/by-nc-nd/4.0/>).

gastric emptying, transit through the small intestine and ultimately, absorption. This model is based on simple mass balances and the description of physiological mechanisms. Our objective is to study the effect of the physical state of the meal on its fate in the gastrointestinal tract. We were inspired by the work of [Marciani et al. \(2012\)](#) in which the gastric emptying of two meals was studied; a meal composed of two phases, one solid and one liquid, or a meal where the solid and liquid components were blended into a homogeneous, single phase. In our model, gastric emptying is described by assuming a constant energy (kcal) delivery into the duodenum compartment and an antral lag time is included to signal the start of antral grinding and gastric emptying for solid meals. To the best of our knowledge, the notion of gastric emptying as a function of the energy density of the digesta has only been explored in one recent model considering computational fluid dynamics within the stomach ([Li & Jin, 2021](#)).

2. Model development

The model assumes that for protein digestion, the gastrointestinal tract can be described with eight compartments, one for the stomach and seven for the small intestine (duodenum, jejunum 1 and 2, ileum 1, 2, 3 and 4, [Fig. 1](#)) ([Yu et al., 1996](#)). The food bolus enters the stomach through the mouth and oesophagus. HCl and pepsin are secreted into the stomach from the parietal and chief cells, respectively. Gastric chyme is emptied from the stomach into the duodenal compartment, where NaHCO_3 and endoproteases such as trypsin, chymotrypsin and elastase are secreted from the pancreas. Chyme continues to flow through the jejunal and ileal compartments. Hydrolysis is simplified by simulating protein hydrolysis into peptides in the stomach and small intestine compartments. Peptide hydrolysis into amino acids (AA) is simulated only from the jejunum 1 to the ileum 4 compartments, assuming that only brush border enzymes have exopeptidase activity and are only present in these compartments. AA are absorbed into and through the enterocytes of the jejunal and ileal compartments into the portal blood. Unabsorbed components flow out of the ileum 4 compartment into the

colon, which is not part of the model anymore.

The primary dependent variables of this model are the quantities or pool sizes, Q_{ij} , of each component, i , in a given compartment, j . These are defined by ordinary differential equations with the independent variable being the time (dQ_{ij}/dt), hence the dynamic nature of the model. The rate of change in the size of each pool is described by the balance between inflows and outflows as depicted in the flow diagram.

2.1. General assumptions and considerations

To construct our model, we assume that the meal arrives in compartments that do not contain nutrients of prior meals. Diffusion is assumed to be instant, for instance, enzymes are in immediate contact with their substrate upon secretion. In the respect of protein or peptide hydrolysis, all peptide bonds are subject to cleavage, i.e. enzyme specificity is not considered.

No processes are modelled past the ileum 4 compartment. Proteic compounds (protein, peptide or AA pools) are considered to be undigested if they arrive in the colon. Likewise, no further metabolism is modelled after AA absorption through the enterocytes into the portal blood. Interindividual variability is not considered.

2.2. Meal characterization

The model considers meals with two possible physical states, one where a solid phase is consumed next to liquid, e.g. water, henceforth referred to as 'solid/liquid' and one where the solid and liquid components form a single, homogeneous phase, this meal is referred to as 'blended' ([Marciani et al., 2012](#)). The composition of the solid/liquid meal is divided into three pools: protein, water, and non-protein/non-water (npnw_5 , representing particles of 5 mm diameter). Meanwhile, the blended meal is described by two pools, protein and non-protein (including water, $\text{np}^{\text{blended}}$, representing the blended meal) pools ([Table 1](#)). To further ease the description of some fluxes, the protein pool is expressed in AA equivalent units. This unit conversion is

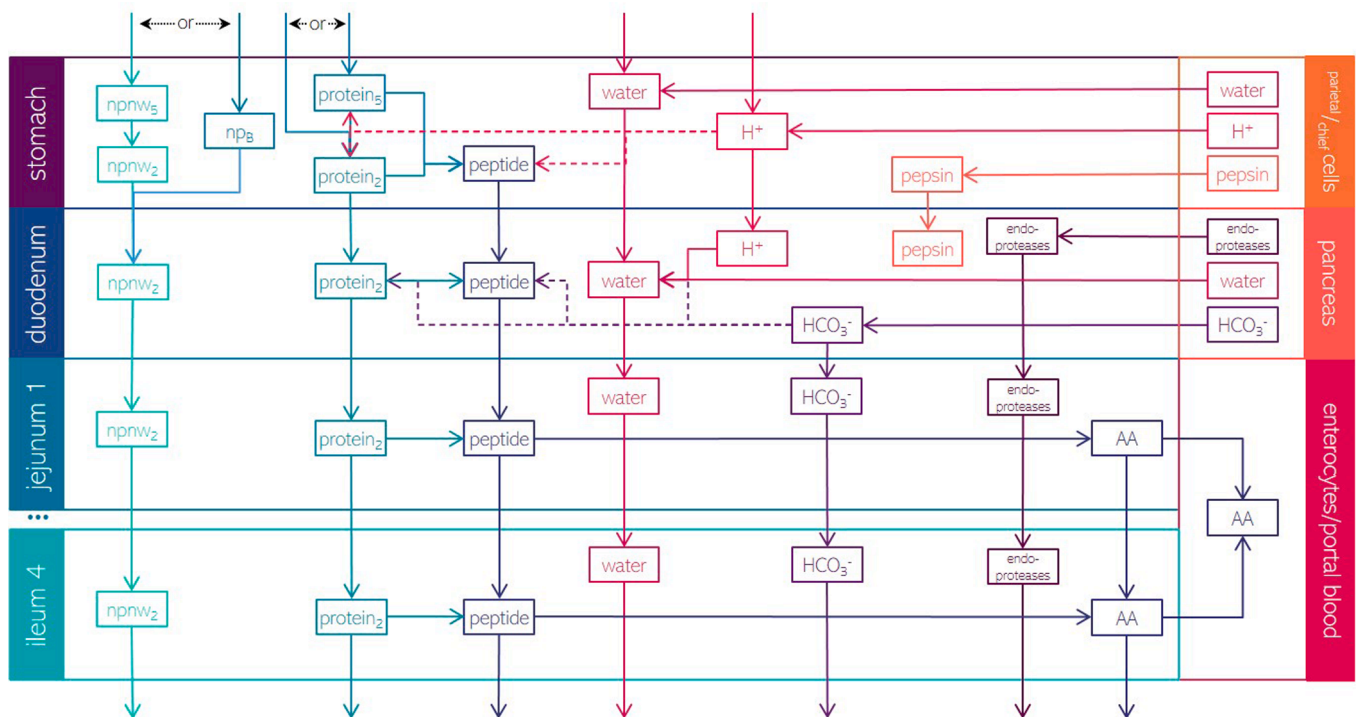


Fig. 1. Flow diagram of the protein digestion model for solid/liquid and blended meals. Solid lines represent fluxes, dashed lines represent influential factors that do not contribute to the protein-peptide mass balance. The jejunum 2, ileum 1, 2 and 3 compartments are not shown but are located after jejunum 1, with the same pools and fluxes as this compartment. npnw₅, non-protein, non-water 5 mm; np_B, non-protein blended; AA, amino acid.

Table 1
Meal properties and composition parameters included in the model description.

| Meal attribute | | Value used in simulation | Unit | | |
|---|-------------------|------------------------------|-----------|------|----------|
| Buffering capacity | | 0.0009 | mmol/l pH | | |
| pH (homogenized meal) | | 5.8 | | | |
| Molecular weight of protein | | 41876.7 | g/mol | | |
| Number of amino acids in sequence | | 377 | aa eq | | |
| Number of glutamic and aspartic acid in protein sequence | | 50 | aa eq | | |
| Number of histidine, glutamic and aspartic acid in protein sequence | | 59 | aa eq | | |
| Rate of food ingestion | | 30 | g/min | | |
| Duration of meal | | 15 | min | | |
| | Solid/liquid meal | Blended meal | | | |
| Composition | water | – | 0.56 | 0 | g/g meal |
| | non-protein | non-protein (water included) | 0.41 | 0.97 | |
| Density | protein | | 0.03 | | g/ml |
| | non-protein | non-protein (water included) | 1.28 | 1.10 | |
| Energetic content | protein | | 1.35 | | kcal/g |
| | non-protein | non-protein (water included) | 0.98 | 0.42 | |
| | protein | | 4 | | |

possible if an average molecular weight and number of AA in the protein sequence is known. In other cases, a representative protein can be chosen to estimate the weight of protein to AA equivalents considering its molecular weight and number of AA in the sequence.

Other meal characteristics required to enter into the model are the pH, the volumetric mass, the energy density of the full meal and its individual pools and the number of AA with pH buffering capacity in the acid and alkaline environment (histidine, glutamic and aspartic acid, Table 1), which can be obtained from the primary structure of the chosen representative protein.

2.3. Intake

A single meal, either solid/liquid or blended, is consumed at a constant rate for the duration of the meal. The solid phase (henceforth called $n_{pnw5\text{ mm}}$ and $protein_{5\text{ mm}}$) of the solid/liquid meal is assumed to be broken down in the mouth into particles of 5 mm diameter.

2.4. Gastric juice secretion

The rate of secretion from the chief and parietal cells of water, pepsin and HCl, into the gastric lumen was modelled as a zero order function triggered by the arrival of bolus into the stomach (Goetze et al., 2009). When the gastric contents of food are lower than 0.5 g, either in the fasted state or after most of the chyme has been emptied into the duodenum, the rate of secretion of gastric juice is assumed marginal.

2.5. Antral grinding

The 5 mm solid particles of the solid/liquid meal ($n_{pnw5\text{ mm}}$ and $protein_{5\text{ mm}}$) that arrive in the stomach compartment are considered too large to pass through the pylorus. We incorporated a lag time between ingestion and the onset of antral contractions and peristalsis into the model (Brown et al., 1993; Houghton et al., 1988). *In vivo*, a lag time has been experimentally observed between ingestion and emptying of solids out of the stomach, and not necessarily of the antral contractions (Camilleri et al., 1985; Siegel et al., 1988). After the lag time (45 min),

antral grinding, i.e. the flux between the 5 mm pools into the 2 mm pools, starts (Fig. 1). This size reduction is described by a zero order function. To signal the end of antral grinding, when most of the large particles have been ground, the flux from the 5 mm pools to the 2 mm pools is then described by a first order rate equation as a function of the remaining $n_{pnw5\text{ mm}}$ and $protein_{5\text{ mm}}$ pools.

2.6. Gastric emptying

Solids are retained in the stomach for a longer period of time compared to liquids. This is known as gastric sieving. Furthermore, many stimuli (mineral acids, fats and fatty acids, osmotic factors, duodenal distension) and receptors in the proximal duodenum and jejunum are involved in inhibiting gastric peristalsis and, as a result, slowing down gastric emptying (Dooley et al., 1984; Roman, 1982; Rønnestad et al., 2014). It has been observed that meals of high energy density are emptied more slowly than meals with lower energy density (Hunt & Stubbs, 1975; Keto et al., 2012). This phenomenological relation between the energy density and the gastric emptying rate probably captures the complex feedback mechanisms that in fact regulate the delivery of chyme into the small intestine. In our model, gastric sieving is accounted for by the lag time to antral grinding and thus gastric emptying of the solid fraction of the solid/liquid meal. Gastric emptying of the non-protein and the other proteic pools ($protein_{2\text{ mm}}$ and peptide) is therefore described by a constant rate of energy delivery into the duodenal compartment (2–2.5 kcal/min) (Hunt et al., 1985). The flux of water, H^+ and pepsin from the stomach into the duodenum compartment are described by zero order kinetics with rate constants for each of the components. When most of the gastric content has been emptied, the flux out of the stomach is described by mass action kinetics with a postprandial gastric emptying rate constant.

2.7. Pancreatic juice secretion

Pancreatic secretion is mediated by various hormonal pathways, triggered by the presence of acid and nutrients in the duodenal lumen, among other stimuli (Pandol, 2011; Vella, 2016). Secretion of pancreatic juice (water, HCO_3^- and endoproteases) into the duodenal compartment is described by zero order kinetics. This flux is prompted by the presence of proteic contents in the duodenum. Secretion starts when the size of the protein and peptide pools combined is larger than 0.1 aa meq, and stops when only this amount remains in the compartment. Endoprotease delivery into the jejunum and ileum compartments results from transit from the duodenum.

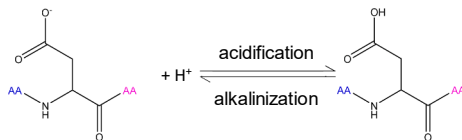
2.8. pH changes

The molar concentration of H^+ in a given compartment was calculated from the balance between inflows, from food and secretions, and outflows, buffering capacity, (de)protonation after hydrolysis, transit and neutralization in the duodenum. Volume of contents within compartments was also calculated dynamically considering the basal volume of gastric or pancreatic juice in a given compartment and the sum of volumes from water, proteic and non-protein pools. As the content in the compartments in this model were considered to be ideally mixed, no spatial differences in pH would be observed within the stomach compartment or small intestine compartments.

– Buffering capacity

The pH in the gastrointestinal tract can be as low as 2, in the fed mid-distal stomach, and as high as 6.7 in the fed mid-distal duodenum (Abuhelwa et al., 2016; Kalantzi et al., 2006; Simonian et al., 2005). The AA with a dissociating side chain having a pKa within this range are histidine (6.5–7.4), aspartic and glutamic acids (4.0–4.8) (Mathews et al., 2000). The buffering rate ($mmol\ H^+ / min$, Eq. (1)), represents the

flow out (or in) of the H^+ pool into (or out of) protein, more specifically the protonatable (or de-protonatable) AA in the structure. However, it is a so called non-additive flux or influential factor to the protein pool, as it does not affect the protein mass balance as such

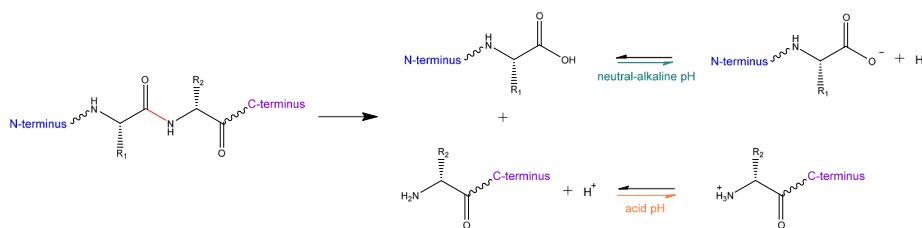


$$\text{Buffering rate} = \frac{k_f Q_{H^+} Q_{B^-}}{Q_w} - k_b Q_A \quad (1)$$

In the acid-base reactions, k_f and k_b (min^{-1}) are the forward and backward rates of buffer reaction ($\text{conjugate base}^- + H^+ \rightleftharpoons \text{weak acid}$) as described by Weinstein et al. (2013). In this expression, Q_{H^+} , Q_{B^-} and Q_A (mmol) are the amounts of protons, deprotonated and protonated amino acid in the protein or peptide sequence, respectively, and Q_w (mmol) is the amount of water.

– (De-)protonation after hydrolysis

A proton is removed or added after a peptide bond cleavage catalysed by pepsin or pancreatic endoproteases, depending on the surrounding pH. A carboxyl and an amino group are released when a peptide bond is hydrolysed. The structure of the resulting peptides influences the pKa of the newly exposed groups. The pKa of $\alpha\text{-COOH}$ is between 3.5 and 4.0, while for $\alpha\text{-NH}_2$ ranges between 8 and 9 (Mathews et al., 2000).



Thus, the flux of protons in or out of the recently exposed carboxyl and/or amino group ($\text{mmol } H^+/\text{min}$) is proposed to be equal to the rate of cleavage itself, i.e., the flux from the protein to the peptide pool (AA eq/min).

– Neutralization of acid chyme

As gastric emptying starts, acidic chyme enters a more alkaline or neutral environment in the duodenum. The bicarbonate already present in the duodenum plus that which begins to be secreted as a result of the presence of nutrients in the compartment neutralizes the acid protons entering in the acid chyme. A water molecule is produced from one molecule of sodium bicarbonate and one of hydrochloric acid. The reaction is correctly balanced with the formation of CO_2 and NaCl , however this is not considered in the model. The neutralization rate (mmol/min) in the duodenum is described by mass action kinetics considering the forward (k_w , mM min^{-1}) and backward (k_o , min^{-1}) rate constants of the neutralization reaction.

$$\text{Neutralization rate}_1 = k_w [H^+]_1 Q_{\text{HCO}_3^-} - k_o Q_{\text{water}} \quad (2)$$

The pH is not calculated beyond the duodenal compartment as any pH-dependency of the global activity of pancreatic proteases is not considered.

2.9. Intestinal transit

The compartmental transit model from Yu et al. (1996) divides the small intestine in seven compartments to better simulate the flow and axial mixing within the organ. This is presented as a suitable compromise between a complex dispersion model and a single compartment one. In the model from Yu et al. (1996), the duodenum represents the first half of the compartment 1, the jejunum the second half along with compartments 2 and 3; and the ileum the remaining four compartments. For simplicity, we consider the complete first compartment to represent the duodenum, the jejunum as compartment 2 and 3 and, the ileum as compartments 4–7.

Transit through the small intestine compartments and out of the ileum 4 into the colon is described by a fractional passage rate with first order kinetics proportional to the pool size of each component in a given compartment. The fractional passage rate is the inverse of the mean retention time which is considered equal for all components of the digesta, in each compartment or the complete small intestine divided by the seven compartments.

2.10. Enzymatic hydrolysis

Protein hydrolysis has been simplified into the conversion from intact protein to peptides, regardless of the size or number of the latter since the proteic pools are modelled as AA equivalents. The protein hydrolysis rate (aa meq/min) in our model depends on a fractional conversion rate (k_E or k_N , mM min^{-1}), the pool size of protein (aa meq) and the concentration of enzyme (mM), considering the dynamicity of the volume of the contents of a given compartment (Eq. (3)).

$$\text{Hydrolysis rate}_{\text{pancreatic endoproteases}} = k_E [\text{endoprotease}]_j Q_{\text{protein}} \quad (3)$$

Furthermore, the activity of digestive proteases depends on the pH (Fersht & Renard, 1974; Goldberg et al., 1969; Hess et al., 1970; Piper & Fenton, 1965). As an aspartic enzyme, pepsin behaves as a diacid and it is active to catalyse hydrolysis in its first deprotonated form. The proportion of the active form of pepsin as a function of pH was expressed by Kondjoyan et al. (2015) and originally derived by Cornish-Bowden and Knowles (1969) (Eq. (4)).

$$X_{\text{pepsin active}} = \frac{1}{1 + \frac{[H^+]}{K_{a1}} + \frac{K_{a2}}{[H^+]}} \quad (4)$$

where K_{a1} and K_{a2} are the first and second dissociation constants. This results in an additional term to Eq. (3) to consider the effect of pH on the pepsin-catalysed hydrolysis rate (aa meq/min).

$$\text{Hydrolysis rate}_{\text{pepsin}} = k_N X_{\text{pepsin active}} [\text{pepsin}]_i Q_{\text{protein}} \quad (5)$$

Residual pepsin activity might continue in the first part of the small intestine while the pH is low enough for the enzyme to be in its active form. Therefore next to hydrolysis in the gastric environment, Eq. (3) and Eq. (5) also express the hydrolysis that might take place in the duodenum.

2.11. Absorption

Peptides are assumed to be small enough to arrive at the brush border and to be the only substrates for exopeptidase-catalysed hydrolysis into single AA in the jejunal and ileal compartments (Fig. 1). The exopeptidase-catalysed hydrolysis is described by first order kinetics, dependent on the amount of peptide present in a given compartment. As AA are produced from the peptide pools, they can diffuse or be transported through the intestinal epithelium. AA absorption is described by Michaelis-Menten-type kinetics to consider the affinity and preference of AA to specific transporters (Bröer, 2008).

2.12. Model simulations

The model was built on the Smart (Simulation and Modelling Assistant for Research and Training) environment (Scholten et al., 1998–2020). This is a user-friendly, free package in which ordinary differential equations can be solved. Once the equations and parameters were entered, simulations were run with the fourth order Runge-Kutta fixed step length numerical integration algorithm with a time step of 6×10^{-4} min, for 420 min. Thorough instructions on the use of Smart have been detailed elsewhere (Gerrits et al., 2021). Model parameters are listed in Table 2; when available, parameters were obtained from literature.

Table 2
Parameter values of the model simulating protein digestion.

| Parameter | Description | Value | Unit | Ref |
|-------------------------------|---|---------|-------------------|------------------------------------|
| <i>Gastric juice</i> | | | | |
| Vs0 | Basal gastric volume | 0.025 | l | Vertzoni et al. (2005) |
| kgj | Rate of gastric juice secretion (fed) | 0.01 | l/min | Versantvoort and Rempelberg (2004) |
| kgjfast | Rate of gastric juice secretion (fasted) | 0.00001 | l/min | |
| Wgj | Water content in gastric juice | 0.999 | l/l | ¹ |
| Hgj | H ⁺ content in gastric juice | 65 | mmol/l | ¹ |
| Ngj | Pepsin(ogen) content in gastric juice | 0.026 | mmol/l | Malagelada et al. (1976) |
| kn | Rate constant of pepsin-catalysed hydrolysis of protein | 60 | min ⁻¹ | ² |
| ka1 | Dissociation constant for first proton pepsin | 0.025 | – | Kondjoyan et al. (2015) |
| ka2 | Dissociation constant of second proton pepsin | 0.003 | – | |
| kfb | Forward rate of buffering | 3000 | ml/meq min | |
| kbb | Backward rate of buffering | 1 | min ⁻¹ | |
| <i>Gastric emptying</i> | | | | |
| antrumlag | Lag time to grinding and gastric emptying of solid bolus | 45 | min | |
| kagNP | Rate of grinding of a non-protein particle from 5 to 2 mm | 1.5 | g/min | |
| kagP | Rate of grinding of a protein particle from 5 to 2 mm | 1.5 | aa meq/min | |
| kge | Rate constant of gastric emptying of food | 2.5 | kcal/min | Hunt and Stubbs (1975) |
| kgeW | Rate constant of gastric emptying of water | 890 | mmol/min | |
| kgeN | Rate constant of gastric emptying of pepsin | 0.00005 | mmol/min | |
| kgeH | Rate constant of gastric emptying of acid | 0.2 | mmol/min | |
| kgepost | Rate constant of postprandial gastric emptying | 0.5 | min ⁻¹ | |
| <i>Pancreatic juice</i> | | | | |
| V10 | Basal duodenal volume | 0.00614 | l | Mudie et al. (2014) ³ |
| pH10 | pH in mid-duodenum (fasted) | 4.9 | – | Ovesen et al. (1986) |
| kpj | Secretion rate of pancreatic juice | 0.004 | l/min | Pandol (2011) |
| Wpj | Water content of pancreatic juice | 0.999 | l/l | |
| Opj | HCO ₃ ⁻ content of pancreatic juice | 300 | mmol/l | |
| kw | Forward rate of neutralization | 100,000 | l/mmol min | |
| ko | Backward rate of neutralization | 0.00001 | min ⁻¹ | |
| Epj | Endoprotease content of pancreatic juice | 13 | mmol/l | |
| ke | Rate constant of endoprotease-catalysed hydrolysis of protein | 15 | l/mmol min | ² |
| <i>Transit and absorption</i> | | | | |
| ksi | Small intestine transit constant | 0.025 | min ⁻¹ | Worsøe et al. (2011) |
| vx | Rate constant of exopeptidase-catalysed hydrolysis | 0.06 | min ⁻¹ | ² |
| vt | Maximum rate of aa transport | 0.03 | aa meq/l min | ² |
| kt | MM constant of aa transport | 0.09 | aa meq/l | ² |

References included for values found in literature, parameter that do not have a reference were based on estimations from calculated values.

¹ Estimated from the composition of gastric juice reported by Malagelada et al. (1976).

² Rates of hydrolysis and absorption represent global, simplified rates from e.g., protein to peptides by all pancreatic endoproteases.

³ Based on the average small bowel resting water volume for the duodenum.

3. Model output

The use of our model to simulate the digestion of protein from solid/liquid and blended meals draws inspiration from the work from Marciani et al. (2012). The participants in this study consumed a solid/liquid meal consisting of chicken, vegetables and water as beverage, or a blended meal consisting of the same components as a homogeneous liquid. The nutrient composition, meal size and duration from this study were used as input to our model. As the main source of protein in this meal is chicken meat, actin was chosen as the representative protein to convert *g protein* into *aa eq* (Murakami & Uchida, 1985; The UniProt Consortium, 2018).

3.1. Gastric phase

3.1.1. Antral grinding

Particles in the food bolus from the solid/liquid meal are considered to be too large to pass through the pylorus. Therefore, a particle size reduction step is included. While it is not clear whether particles are ground during this retention time, in our model, grinding starts after an ‘antrum lag’ and, consequently, also gastric emptying of the ground particles. Fig. 2 shows, first, the ingestion of 185 g of the non-protein, non-water fraction of the meal, over 15 min. Second, the ‘antrum lag’, during which there is virtually no change in the pool size of 5 mm particles (Qnpnw₅) for 30 min after ingestion. Third, the flux from npnw_{5 mm} to npnw_{2 mm} starts (Fig. 1), as indicated by the reduction in the 5 mm pool or the increase in the cumulative pool of ground material.

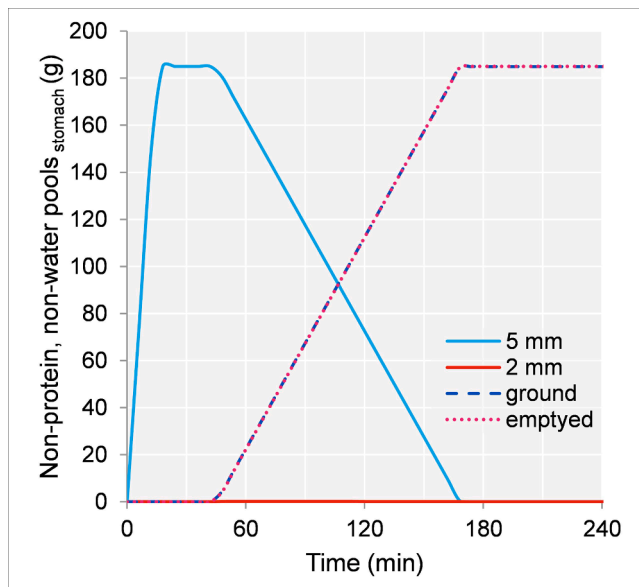


Fig. 2. Simulated antral grinding of 5 mm particles and gastric emptying of 2 mm particles from the solid/liquid meal. Solid lines indicate absolute pools of 5 and 2 mm non-protein particles, dashed lines indicate cumulative pools of ground and emptied particles.

Small particles are emptied out of the stomach as soon as they appear. This results in a very small pool size of 2 mm particles and in an overlap of the cumulative pools of ground and emptied material.

3.1.2. Gastric emptying

Gastric emptying is described by a constant delivery of calories into the duodenum compartment from the nutrient pools (2 mm or blended). Meanwhile water, being a non-caloric component, was described with an independent emptying rate (explained by gastric sieving and also the so called Magenstrasse effect (Pal et al., 2007)). It should be noted that in our model, the water from the gastric juice secretion contributes to the water pool in the stomach. To show these effects, we calculated the volume of the contents in the stomach compartment (Fig. 3). After ingestion of the solid/liquid meal, gastric emptying showed a two-phase character. Water is emptied as soon as the meal is ingested, while the

emptying of solids is delayed by the ‘antrum lag’. As antral grinding starts, so does the emptying of nutrients.

The blended meal was emptied at a constant rate for most of the duration of the gastric phase. This meal is emptied at a faster rate than that of the solids from the solid/liquid meal because of its lower caloric density. Regardless, the volume of gastric contents was higher from the blended meal than from the solid/liquid meal due to the fast emptying of water.

Including the ‘antrum lag’ and describing the gastric emptying of nutrients in terms of calories delivered to the duodenum allows us to mimic the biphasic nature of gastric emptying of a solid/liquid meal and the monophasic nature of homogenized liquid meals as presented in Fig. 3 (Marciani et al., 2012; Siegel et al., 1988). Nevertheless, in the study of Marciani et al. (2012), gastric content from both meals were emptied over a similar period of time (ca. 170 min). From our simulation, most of the contents of the stomach compartment from the blended meal are emptied nearly an hour before they are for the solid/liquid meal, suggesting that there are more phenomena that determine the duration of the gastric phase than those that are currently described in our model.

3.1.3. pH of gastric content

The contents within each compartment are assumed to be instantly mixed. Thus, a single pH throughout the stomach is estimated based on the inflows of H^+ , (1) from the meal which is rather marginal, (2) from the basal gastric juice content from the fasted state and, more significantly, (3) from the secretion of gastric juice in the fed state (Fig. 1). The outflows are (1) the buffering capacity of the protein, (2) the protonation after protein hydrolysis and (3) gastric emptying of acid into the duodenum compartment. The volume of the gastric contents is considered to be dynamic and changing with time, which of course also affects the calculation of the H^+ concentration.

Gastric juice secretion is stimulated by the presence of nutrients in the stomach compartment. A basal volume of gastric juice, including acid, is present in the fasted state (Fig. 4, time 0), even though the amount of basal gastric juice is negligible compared to the fed state secretion as can be observed in the following time points. It can be seen for the solid/liquid meal that secretion proceeds until 180 min, whereas it reaches a maximum at 120 min for the blended meal. The end of the fed secretion rate corresponds to the moment when most of the gastric contents have been emptied out, which for the solid/liquid meal, is related to the assumed rate of breakdown of larger particles and the

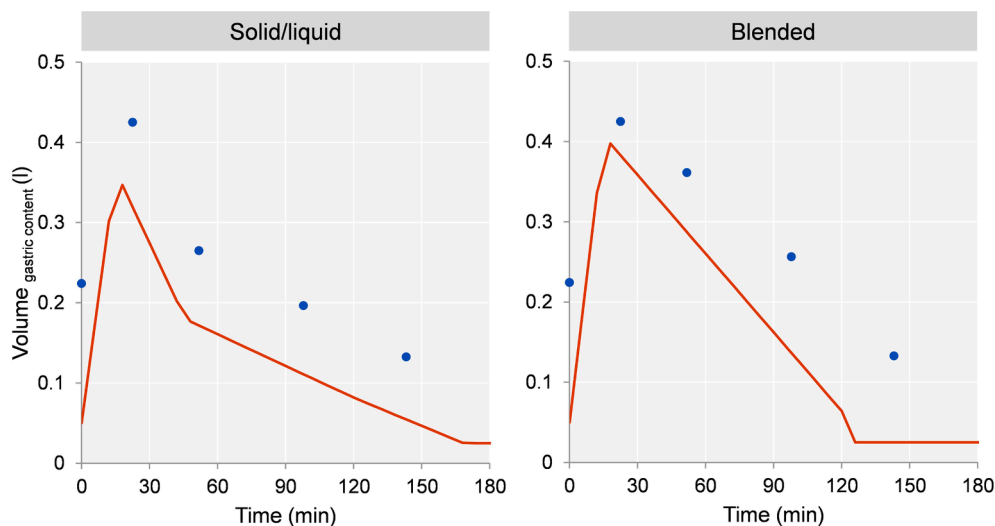


Fig. 3. Volume of gastric content from solid/liquid and blended meals, model output in orange and data points from Marciani et al. (2012) in blue. Note that the model was not fitted. Time zero indicates the time of meal ingestion. (For interpretation of the references to colour in this figure legend, the reader is referred to the web version of this article.)

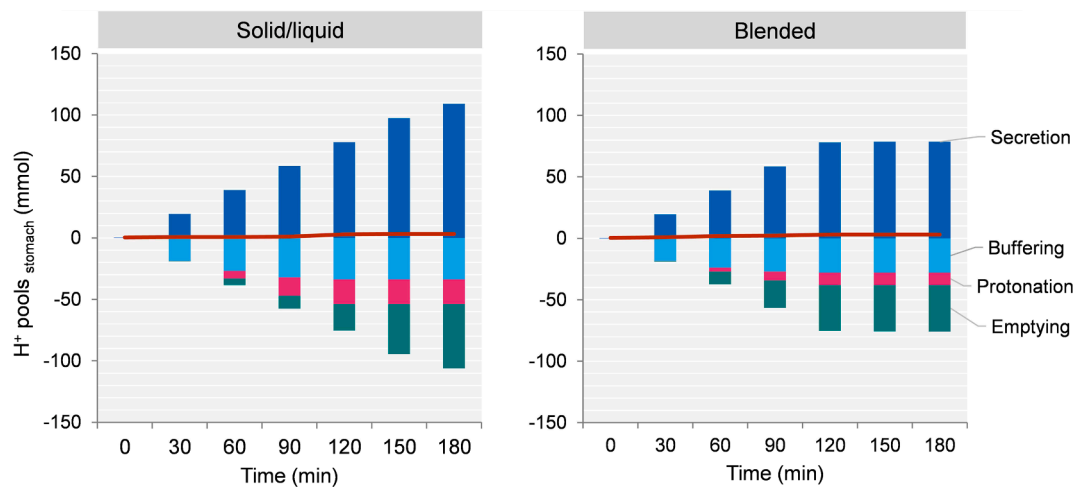


Fig. 4. Cumulative pools from the in and out fluxes of the H^+ pool (bars) and absolute H^+ pool (line) in the stomach compartment from solid/liquid and blended meals.

gastric emptying of the smaller ones. Afterwards, it returns to a post-prandial or fasted secretion rate which is much lower.

The most significant outflux from the H^+ pool at the beginning of the gastric phase is the protonation of acidic AA, which accounts for the proteins' buffering capacity. This outflux increases slightly after 30 min, i.e. most of the buffering capacity is expressed as soon as the protein is ingested. It is assumed that all binding sites are exposed instantaneously after having been ingested, and readily available for protonation. By incorporating a diffusion term, the buffering capacity could be more realistically represented as a sustained flux for a longer period of time. A more sophisticated empirical model to predict the buffering capacity of protein gels and dispersions was proposed by [Mennah-Govela et al. \(2019\)](#). That model accounts for the exposure of acidic amino acids by considering the surface area of particles. For simplicity, this model was not used as it considers diffusion phenomena and requires a number of fitting parameters as well as an accurate characterization of the protein's amino acid profile.

The protonation flux belongs to the more interesting ones as the pepsin activity is influenced by the concentration of H^+ , and protonation after pepsin-catalysed hydrolysis influences the H^+ pool. As will be discussed further, the pepsin-catalysed hydrolysis of protein progresses along the gastric phase, in part because of the decreasing pH, and hence the protonation of the resulting amino groups does as well. Less protonation was recorded for the blended meal reflecting a lower extent of protein hydrolysis.

Lastly, the gastric emptying of acid also influences the concentration of H^+ in the gastric contents. More acid is emptied from the stomach compartment during the digestion of the solid/liquid meal. This is again explained by the retention of the gastric contents for a longer period for this meal than for the blended meal, as the acid emptying rate constant is higher in the fed state than in the fasted state as a proxy for the overall emptying of chyme.

The pH resulting from the contribution of these fluxes to the H^+ pool as well as the dynamic volume of the gastric contents shows a different profile for the two meals ([Fig. 5](#)). For both meals, the initial increase results from the meal ingestion and dilution of the basal gastric juice present in the compartment. Our results follow a trend qualitatively similar to that observed by [Malagelada et al. \(1979\)](#) as the bolus from the blended meal reaches a higher pH than that from the solid/liquid meal. The sharp decrease can be associated to both the onset of gastric secretions but also to the reduction of the gastric volume. The pH reduction is dampened by the protein's buffering capacity but more significantly by the start of the pepsin-catalysed hydrolysis. This continues until the end of the gastric phase or when most of the contents have been emptied. At this point, both the secretion and emptying slow down and the pH remains relatively constant. Unlike the results from ([Malagelada et al.](#)), the pH of the solid/liquid meal is consistently higher than that from the blended meal during the acidification of the gastric chyme.

The concept of the gastric pH, just as that of other compartments, is

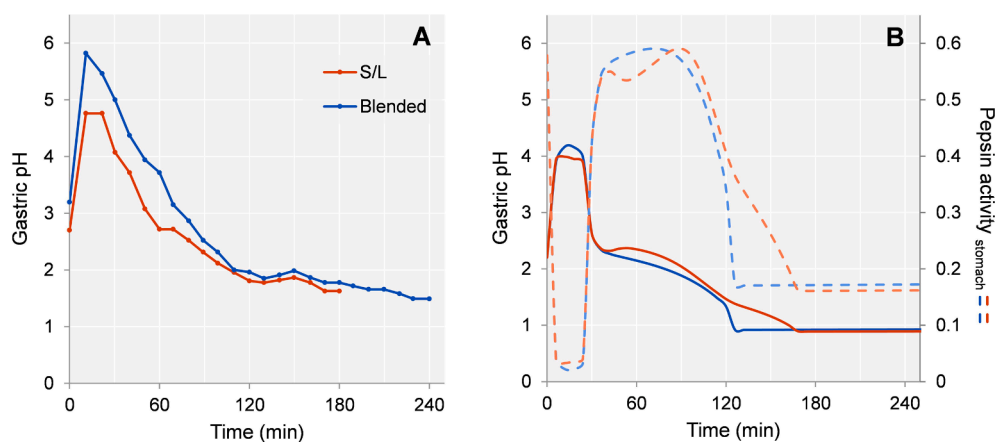


Fig. 5. pH of gastric contents from solid/liquid and blended meals, (A) data points from [Malagelada et al. \(1979\)](#), (B) model output: pH (solid lines) and, fractional pepsin in its active form (dashed lines).

rather ambiguous. It is known that pH in the stomach not only changes over time but also spatially throughout the stomach (Bornhorst et al., 2014; Simonian et al., 2005) and even within particles (van der Sman et al., 2020). Furthermore, pH will also be heterogeneous within the digesta composed of solid particles of various sizes, a liquid phase from the meal and the gastric juice. A potential approach to describe the local pHs could be to fragment the stomach compartment into several sub-compartments with their own H^+ pools and fluxes. Le Feunteun et al. (2014), for example, described the stomach as two compartments instead of one and simulated the secretion rate of the gastric juice using a gaussian step function.

– Pepsin activity.

The pH influences the amount of pepsin that is in its active form. Fig. 5 shows the time interval at which pepsin is most active, i.e. when the highest possible proportion of pepsin is in its active form. In the first 30 min, when the pH is the highest, a very small fraction of pepsin is active. As the pH drops sharply, the pepsin activity increases and its maintained roughly between pH 2.2 and 1.7. When pH decreases further until ca. 1, the pepsin activity drops accordingly.

3.2. Small intestinal phase

3.2.1. pH of duodenal contents

The influx to the H^+ pool in the duodenum compartment is the gastric emptying of acid chyme. The outfluxes are the protonation after protein hydrolysis (if $pH < 5$) and neutralisation by the bicarbonate secreted in the pancreatic juice. As in the gastric phase, the pH profile of the duodenal contents shows the interplay of many events occurring in the gastrointestinal tract (Fig. 6A and B). Acid chyme arrives in the duodenum compartment increasing the size of the H^+ pool and causing the pH to drop.

In our model, pancreatic secretion is stimulated by the presence of proteic (protein and/or peptide) pools in the duodenum compartment. Protein from the solid/liquid meal must be ground in the stomach before it can be emptied into the duodenum, but $protein_{5\text{ mm}}$ is subject to pepsin-catalysed hydrolysis from the moment of ingestion. The resulting peptides can flow out of the stomach as they are being formed. However,

only a small part of pepsin is in its active form during the first minutes of the gastric phase because of the relatively high pH. Thus, virtually no peptides are formed initially. In sum, the physical state of the meal and the pH of the gastric content cause pancreatic secretion to start only ca. 30 min after the meal has started. It is only then that the pH starts to return to the basal pH of the duodenum. Conversely, the pH of the duodenal contents from the blended meal does not show a significant drop, as the protein arrives earlier in the duodenum and, as a result, the pancreatic secretion starts earlier than in the case of the solid/liquid meal (Fig. 6B point 1).

The pH is roughly constant for 60–120 min for the solid/liquid meal, and until 90 min for the blended meal. Afterwards, the pH decreases. These times coincide with the onset of a progressively slower rate of protein hydrolysis in the duodenum compartment (Fig. S1). H^+ accumulates as there is less protonation after protein hydrolysis, and the pancreatic juice secretion is not sufficient to neutralize the incoming acid from the stomach compartment. This pH drop continues until most of the gastric contents have been emptied, and the gastric secretion and emptying slows down.

3.2.2. Secretion of pancreatic endoproteases

Endoproteases are secreted from the pancreas into the duodenum along with HCO_3^- and water. As described for HCO_3^- secretion, endoprotease secretion starts as proteic components arrive in the duodenum compartment. Fig. 6C and D show the onset of pancreatic endoprotease secretion occurring earlier for the blended than the solid/liquid meal. This relates to the gallbladder contraction observations from Marciani et al. (2012), which were greater for the blended meal and thus expected to induce a higher pancreatic secretory response than the solid/liquid meal. For the solid/liquid meal, the onset of pancreatic secretions is stimulated by the arrival of peptides from protein hydrolysis in the stomach.

The pancreatic juice is modelled to only be secreted into the duodenum (Fig. 1). The endoproteases flow from the duodenum through the jejunum and ileum compartments along with the rest of the digesta. Besides the onset of pancreatic juice secretion, no major differences emerge from the intake of the two types of meals on the size of the endoprotease pools in the small intestine compartments. The secretion of pancreatic juice stops when most of the proteic pools have flowed out

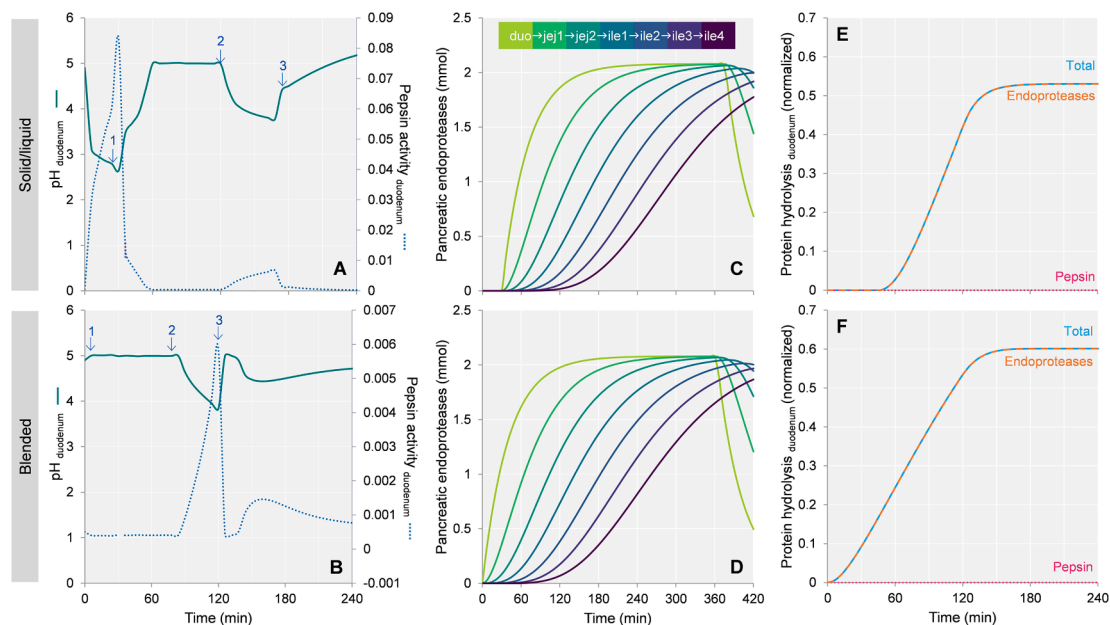


Fig. 6. (A-B) pH and pepsin activity in the duodenum compartment, (1) start of pancreatic juice secretion, (2) maximum rate of protein hydrolysis in duodenum compartment, (3) end of gastric secretion in the fed state. (C-D) Pancreatic endoproteases in the small intestine compartments. (E-F) Protein hydrolysis in the duodenum, contribution from pepsin and endoproteases.

of the duodenum into the jejunum 1 compartment (Fig. S2).

As previously discussed, the pepsin activity depends on the pH of the medium. Some residual pepsin-catalysed hydrolysis could be observed in the duodenum, as both pepsin and acid are emptied within the chyme from the stomach compartment. However, the fraction of active enzyme is considerably lower in the duodenum than in the stomach compartment (Fig. 6A and B). As a result, pepsin-catalysed hydrolysis is virtually non-existent in the duodenum and nearly all of the protein hydrolysis occurs due to the action of pancreatic endoproteases (Fig. 6E and F).

3.3. Transit of proteic pools

The compartmental modelling allows monitoring of the concentration of a given component in a given compartment at any moment in time during digestion. Fig. 7 shows the transit and appearance of the intact protein, peptide and AA pools throughout the stomach, small intestine and portal blood compartments. As previously discussed, the solid protein in the solid/liquid meal is retained for a longer time in the stomach compartment than the protein in the blended meal. Interestingly, peptides resulting from pepsin-catalysed hydrolysis in the stomach from the blended meal accumulate in this compartment and are retained longer than those from the solid/liquid meal. As large particles are retained in the stomach during the ‘antrum lag’, peptides from the solid/liquid meal are the only nutrients that can be emptied out of the stomach (Fig. S3). Meanwhile, for the blended meal, non-protein, protein and peptides are emptied at the same time. Peptides, therefore, accumulate in the stomach compartment since proteins are hydrolysed and emptied at a slower rate, compared to those from the solid/liquid meal.

The earlier arrival into the duodenum of protein from the blended meal also implies earlier formation of peptides in the small intestine compartments. When protein arrives in the duodenum compartment, it initially accumulates as the rate of gastric emptying is higher than that of the protein hydrolysis in the duodenum, while the transit into the following small intestine compartment, jejunum 1 is still zero.

The exopeptidases that catalyse the hydrolysis of peptides into AA are located in the jejunum and ileum compartments. It can be seen that there is very little accumulation of AA in the jejunum and ileum compartments. This is because the AA are quickly absorbed by the enterocytes as soon as they are being formed (Fig. S4). As expected, the onset of the AA absorption fluxes from the jejunum 1 to ileum 4 compartments

into the portal blood starts earlier for the blended than for the solid/liquid meal.

3.4. Protein hydrolysis

From our model, pepsin-catalysed hydrolysis is particularly significant as many events influence its extent and rate, i.e. enzyme and substrate (5 mm, 2 mm or blended) concentration in the compartment, and pH, which is in turn influenced by protonation after protein hydrolysis (Fig. S5). We observe that protein hydrolysis does not start until about 15 min after either meal has been ingested. This is explained by the high pH, thus low proportion of pepsin in its active form, as well as the dynamic secretion of pepsin in the gastric juice.

The physical state of the meal influences protein hydrolysis, and more specifically, the extent of protein hydrolysis in a given compartment. A longer residence time in the stomach, e.g. for the solid/liquid meal where more protein is retained, results in a higher degree of hydrolysis than a shorter residence time (Fig. 8). For the blended meal, a small fraction of the protein is hydrolysed in the stomach compartment. Nevertheless, protein hydrolysis in the duodenum compensates for these differences. A similar extent of hydrolysis is achieved by the end of the duodenal phase for both meals, granted that the start and end of protein hydrolysis in the duodenum occur earlier for the blended meal. Most hydrolysis takes place in the duodenum, since protein hydrolysis is described by mass action kinetics from both the substrate and the enzyme, even though the initial hydrolysis in the stomach is crucial as it liquifies the digesta and makes it available for further hydrolysis.

We have previously reported on the influence of the pH and hydrolysis history of proteins and peptides during the gastric phase on the extent and efficiency of subsequent hydrolysis of trypsin in small intestinal conditions (Rivera del Rio et al., 2021). This influence was not considered in the current model, it would however be interesting to incorporate in further versions.

Similarly, the fraction of peptides that is hydrolysed is highest in the jejunum 1 compartment, with respect to the other jejunum and ileum compartments. Because of the earlier arrival of protein from the blended meal into this compartment, peptide hydrolysis into AA as well as AA absorption, occurs earlier than for the solid/liquid meal. However, the extent of hydrolysis and absorption is similar with both meals.

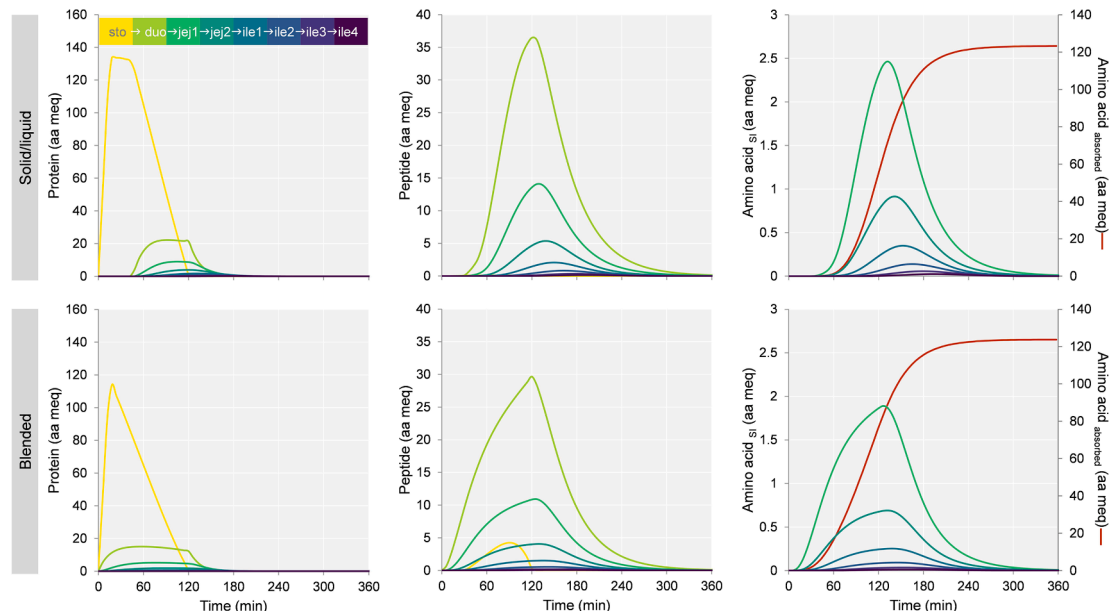


Fig. 7. Simulated proteic (protein, peptide and amino acid) pools in the stomach, small intestine and portal blood compartments.

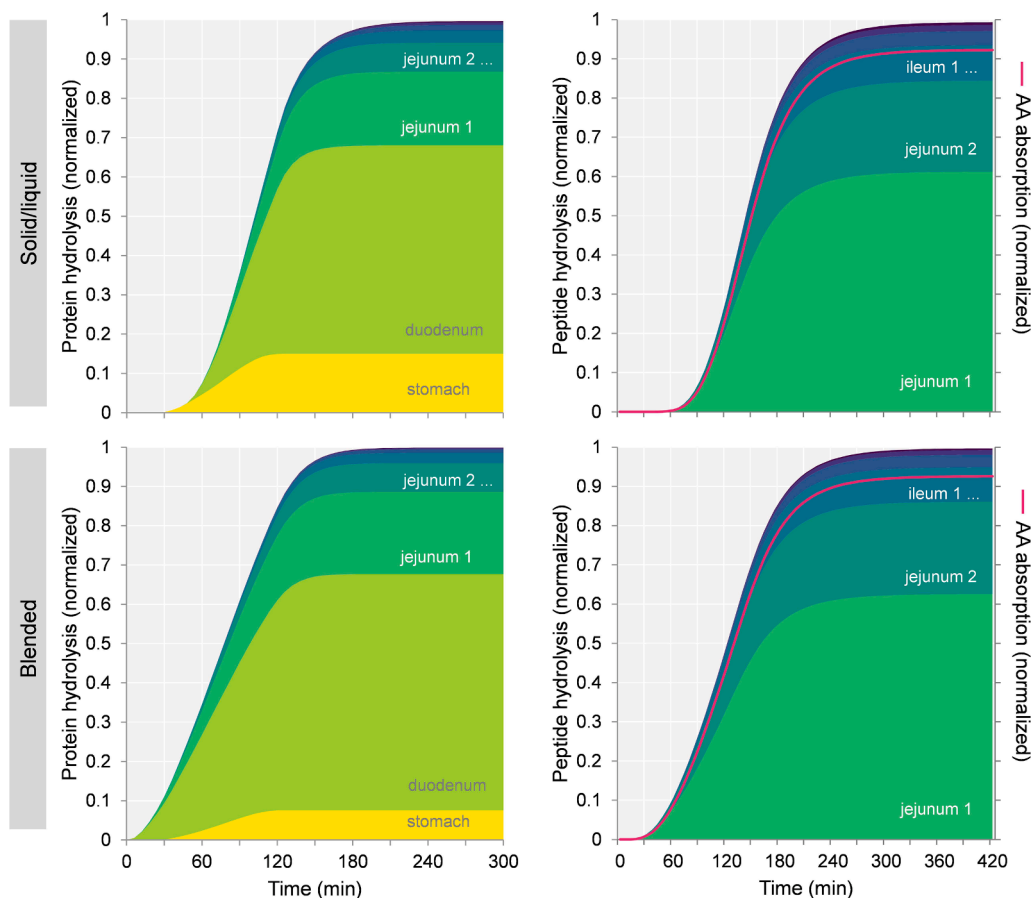


Fig. 8. Simulated protein hydrolysis into peptides by pepsin and pancreatic endoproteases, peptide hydrolysis into amino acids by brush border exopeptidases, and cumulative pool of absorbed amino acids. Pools are normalized to the total amount of protein consumed.

3.5. AA absorption

Effectively, the AA absorption curves depicted in Fig. 7 and Fig. 8 represent the disappearance of AA from the small intestine. This can be compared to the measure of true ileal digestibility, which has been reported to be ca. 92% for chicken meat, similar to the outcome of the model (Faber et al., 2010; Kashyap et al., 2018). The proteic content (protein, peptide and AA) that is not absorbed through the enterocytes, flows into the colon and is virtually lost for AA utilization.

Naturally, the absorbed AA do not accumulate in the portal blood. It is difficult to compare the rate of AA absorption from our model to that occurring *in vivo*. The AA metabolism has been reported to start already in the intestinal tissues during absorption, the so called first-pass metabolism (van der Schoor et al., 2002). The AA are utilized to maintain the gut mucosa, to generate intestinal energy and for oxidative purposes, before they are available for whole-body metabolism. Schop et al. (2020) argue that the quality of the net portal appearance of AA data available is insufficient to compare to simulated AA absorption kinetics.

In vitro experimental methods are advanced enough to mimic protein hydrolysis in the small intestinal lumen, however the action of brush border enzymes as well as absorption into and through enterocytes are not readily available to apply in a laboratory setting. Furthermore, predicting the effect of passage is easier when done through an *in silico* model, compared to a static or semi-dynamic *in vitro* setting. An *in silico* approach as the one presented in this work can complement the *in vitro* observations, simulating complex processes during food digestion.

3.6. Future perspectives

The current model relies on several parameters (Table 2), some were obtained from literature while others were estimated to simulate digestive processes. To better inform these estimated values some experimental work is still required. For instance, parameters influencing pH, such as forward and backward rates of buffering or neutralization should be determined in realistic *in vitro* digestion media.

Future versions of the model should incorporate more aspects that influence gastric emptying, beyond caloric density and physical state of the meal. Protein properties also influence gastric emptying. It is well known that milk proteins show different behaviour in the gastrointestinal tract; whey proteins are quickly emptied from the stomach, while casein coagulates and is emptied later and more slowly than whey proteins (Boirie et al., 1997; Huppertz & Chia, 2021).

The composition and rheological properties of chyme are also relevant to the gastric emptying rate. For instance, it was reported that the source of the calories, i.e., from proteins, carbohydrates or fats, influences the rate of gastric emptying. Giezenaar et al. (2018) found that the rate of calorie delivery to the duodenum in the first 60 min after ingestion was 2.7 kcal/min for a drink with whey protein. An isocaloric drink with whey protein, dextrose and olive oil was emptied approximately 1.4 times faster.

The presence of dietary fibre delays and slows down the gastric emptying of protein (Bornhorst et al., 2013). This was associated to layering within the stomach of brown rice bran fragments in the antrum. Interestingly, this effect was only observed for protein and not for starch or dry matter. Further, the viscosity of chyme has been reported to be inversely related to the rate of gastric emptying and overall transit through the gastrointestinal tract (Darwiche, Björge, & Almér, 2003;

Ménard et al., 2018).

4. Concluding remarks

An adequate representation of the gut physiology is required to study the relevance of the physical state of meals. We chose for a dynamic, semi-mechanistic, compartmental model to describe protein digestion. The components of the digesta that were deemed most relevant for protein digestion were included. Fluxes between pools were described by simple functions with a physiological meaning.

The model uses the Smart environment for computation, which is a free and user friendly tool that is suitable as a first step into *in silico* modelling. The qualitative agreement with experiments on gastric pH and volume of the gastric contents is good considering that the model consists of independent equations and was not fitted to the data. Extensions and testing against experimental observations will improve the predicted accuracy and versatility of the model.

The model was applied to investigate the influence of the physical state of meals and was examined on transit, digestive protein hydrolysis, and amino acid absorption. The digesta from the blended meal was emptied first and faster from the stomach, compared to that of the solid/liquid meal. The model was able to simulate the biphasic nature of gastric emptying from solid/liquid meals as reported from *in vivo* trials. Furthermore, we show the dynamic behaviour of the pH and its effect on the enzymatic protein hydrolysis, both in gastric as well as the duodenal environment.

Funding

This work was supported by the Consejo Nacional de Ciencia y Tecnología, Mexico [grant number 480085].

CRedit authorship contribution statement

Andrea Rivera del Rio: Conceptualization, Investigation, Methodology, Visualization, Writing – original draft. **Nikkie van der Wielen:** Investigation, Methodology, Writing – review & editing. **Walter J.J. Gerrits:** Conceptualization, Methodology, Writing – review & editing. **Remko M. Boom:** Methodology, Writing – review & editing. **Anja E.M. Janssen:** Conceptualization, Methodology, Supervision, Writing – review & editing.

Declaration of Competing Interest

The authors declare that they have no known competing financial interests or personal relationships that could have appeared to influence the work reported in this paper.

Appendix A. Supplementary material

Supplementary data to this article can be found online at <https://doi.org/10.1016/j.foodres.2022.111271>.

References

- Abuhelwa, A. Y., Foster, D. J., & Upton, R. N. (2016). A quantitative review and meta-models of the variability and factors affecting oral drug absorption—part I: Gastrointestinal pH. *The AAPS Journal*, 18(5), 1309–1321. <https://doi.org/10.1208/s12248-016-9952-8>
- Bastianelli, D., Sauvant, D., & Rérat, A. (1996). Mathematical modeling of digestion and nutrient absorption in pigs. *Journal of Animal Science*, 74(8), 1873–1887. <https://doi.org/10.2527/1996.7481873x>
- Boirie, Y., Dangin, M., Gachon, P., Vasson, M.-P., Maubois, J.-L., & Beaufrère, B. (1997). Slow and fast dietary proteins differently modulate postprandial protein accretion. *Proceedings of the National Academy of Sciences*, 94(26), 14930–14935. <https://doi.org/10.1073/pnas.94.26.14930>
- Bornhorst, G. M., Chang, L. Q., Rutherford, S. M., Moughan, P. J., & Singh, R. P. (2013). Gastric emptying rate and chyme characteristics for cooked brown and white rice

- meals in vivo. *Journal of the Science of Food and Agriculture*, 93(12), 2900–2908. <https://doi.org/10.1002/jsfa.6160>
- Bornhorst, G. M., Rutherford, S. M., Roman, M. J., Burri, B. J., Moughan, P. J., & Singh, R. P. (2014). Gastric pH distribution and mixing of soft and rigid food particles in the stomach using a dual-marker technique. *Food Biophysics*, 9(3), 292–300. <https://doi.org/10.1007/s11483-014-9354-3>
- Brøer, S. (2008). Amino acid transport across mammalian intestinal and renal epithelia. *Physiological Reviews*, 88(1), 249–286. <https://doi.org/10.1152/physrev.00018.2006>
- Brown, B. P., Schulze-Delrieu, K., Schrier, J. E., & Abu-Yousef, M. M. (1993). The configuration of the human gastroduodenal junction in the separate emptying of liquids and solids. *Gastroenterology*, 105(2), 433–440. <https://doi.org/10.5555/uri:pii:001650859390717Q>
- Camilleri, M., Malagelada, J., Brown, M., Becker, G., & Zinsmeister, A. (1985). Relation between antral motility and gastric emptying of solids and liquids in humans. *American Journal of Physiology-Gastrointestinal and Liver Physiology*, 249(5), G580–G585. <https://doi.org/10.1152/ajpgi.1985.249.5.G580>
- Cornish-Bowden, A. J., & Knowles, J. R. (1969). The pH-dependence of pepsin-catalysed reactions. *The Biochemical Journal*, 113(2), 353–362. <https://doi.org/10.1042/bj1130353>
- Darwiche, G., Björgell, O., & Almér, L.-O. (2003). The addition of locust bean gum but not water delayed the gastric emptying rate of a nutrient semisolid meal in healthy subjects. *BMC Gastroenterology*, 3(1), 12. <https://doi.org/10.1186/1471-230X-3-12>
- Dooley, C. P., Reznick, J. B., & Valenzuela, J. E. (1984). Variations in gastric and duodenal motility during gastric emptying of liquid meals in humans. *Gastroenterology*, 87(5), 1114–1119. [https://doi.org/10.1016/S0016-5085\(84\)80071-2](https://doi.org/10.1016/S0016-5085(84)80071-2)
- Faber, T. A., Bechtel, P. J., Hernot, D. C., Parsons, C. M., Swanson, K. S., Smiley, S., & Fahey, G. C., Jr. (2010). Protein digestibility evaluations of meat and fish substrates using laboratory, avian, and ileally cannulated dog assays. *Journal of Animal Science*, 88(4), 1421–1432. <https://doi.org/10.2527/jas.2009-2140>
- Fersht, A. R., & Renard, M. (1974). pH Dependence of chymotrypsin catalysis. Appendix. Substrate binding to dimeric α -chymotrypsin studied by X-ray diffraction and the equilibrium method. *Biochemistry*, 13(7), 1416–1426. <https://doi.org/10.1021/bi00704a016>
- Gerrits, W. J. J., Schop, M. T. A., de Vries, S., & Dijkstra, J. (2021). ASAS-NANP symposium: Digestion kinetics in pigs: The next step in feed evaluation and a ready-to-use modeling exercise. *Journal of Animal Science*, 99(2). <https://doi.org/10.1093/jas/skab020>
- Giezenaar, C., Lange, K., Hausken, T., Jones, K. L., Horowitz, M., Chapman, I., & Soenen, S. (2018). Acute effects of substitution, and addition, of carbohydrates and fat to protein on gastric emptying, blood glucose, gut hormones, appetite, and energy intake. *Nutrients*, 10(10), 1451. <https://doi.org/10.3390/nu10101451>
- Goetze, O., Treier, R., Fox, M., Steingoetter, A., Fried, M., Boesiger, P., & Schwizer, W. (2009). The effect of gastric secretion on gastric physiology and emptying in the fasted and fed state assessed by magnetic resonance imaging. *Neurogastroenterology & Motility*, 21(7), 725–e742. <https://doi.org/10.1111/j.1365-2982.2009.01293.x>
- Goldberg, D., Campbell, R., & Roy, A. (1969). Fate of trypsin and chymotrypsin in the human small intestine. *Gut*, 10(6), 477. <https://doi.org/10.1136/gut.10.6.477>
- Halas, V., Gerrits, W. J., & van Milgen, J. (2018). Models of feed utilization and growth for monogastric animals. In: Wagenigen Academic Publishers, The Netherlands.
- Hess, G., McConn, J., Ku, E., & McConkey, G. (1970). Studies of the activity of chymotrypsin. *Philosophical Transactions of the Royal Society of London B, Biological Sciences*, 257(813), 89–104. <https://doi.org/10.1098/rstb.1970.0011>
- Houghton, L. A., Read, N. W., Heddle, R., Horowitz, M., Collins, P. J., Chatterton, B., & Dent, J. (1988). Relationship of the motor activity of the antrum, pylorus, and duodenum to gastric emptying of a solid-liquid mixed meal. *Gastroenterology*, 94(6), 1285–1291. <https://doi.org/10.5555/uri:pii:0016508588906658>
- Hunt, J., Smith, J., & Jiang, C. (1985). Effect of meal volume and energy density on the gastric emptying of carbohydrates. *Gastroenterology*, 89(6), 1326–1330. [https://doi.org/10.1016/0016-5085\(85\)90650-x](https://doi.org/10.1016/0016-5085(85)90650-x)
- Hunt, J., & Stubbs, D. (1975). The volume and energy content of meals as determinants of gastric emptying. *The Journal of physiology*, 245(1), 209–225. <https://doi.org/10.1113/jphysiol.1975.sp010841>
- Huppertz, T., & Chia, L. W. (2021). Milk protein coagulation under gastric conditions: A review. *International Dairy Journal*, 113, 104882. <https://doi.org/10.1016/j.idairyj.2020.104882>
- Kalantzi, L., Goumas, K., Kalioras, V., Abrahamsson, B., Dressman, J. B., & Reppas, C. (2006). Characterization of the human upper gastrointestinal contents under conditions simulating bioavailability/bioequivalence studies. *Pharmaceutical Research*, 23(1), 165–176. <https://doi.org/10.1007/s11095-005-8476-1>
- Kashyap, S., Shivakumar, N., Varkey, A., Duraisamy, R., Thomas, T., Preston, T., Devi, S., & Kurpad, A. V. (2018). Ileal digestibility of intrinsically labeled hen's egg and meat protein determined with the dual stable isotope tracer method in Indian adults. *The American Journal of Clinical Nutrition*, 108(5), 980–987. <https://doi.org/10.1093/ajcn/nqy178>
- Keto, Y., Hirata, T., Takemoto, Y., Yamano, M., & Yokoyama, T. (2012). Influence of gastric acid on gastric emptying and gastric distension-induced pain response in rats—effects of famotidine and mosapride. *Neurogastroenterology & Motility*, 24(2), 147–e188. <https://doi.org/10.1111/j.1365-2982.2011.01809.x>
- Kondjoyan, A., Daudin, J.-D., & Santé-Lhoutellier, V. (2015). Modelling of pepsin digestibility of myofibrillar proteins and of variations due to heating. *Food Chemistry*, 172, 265–271. <https://doi.org/10.1016/j.foodchem.2014.08.110>
- Le Feunteun, S., Al-Razaz, A., Dekker, M., George, E., Laroche, B., & van Aken, G. (2021). Physiologically based modeling of food digestion and intestinal microbiota: state of the art and future challenges. An INFOGEST review. *Annual Review of Food Science*

- and Technology, 12(1), 149–167. <https://doi.org/10.1146/annurev-food-070620-124140>
- Le Feunteun, S., Barbé, F., Rémond, D., Ménard, O., Le Gouar, Y., Dupont, D., & Laroche, B. (2014). Impact of the dairy matrix structure on milk protein digestion kinetics: Mechanistic modelling based on mini-pig in vivo data. *Food and Bioprocess Technology*, 7(4), 1099–1113. <https://doi.org/10.1007/s11947-013-1116-6>
- Le Feunteun, S., Mackie, A. R., & Dupont, D. (2020). In silico trials of food digestion and absorption: How far are we? *Current Opinion in Food Science*. <https://doi.org/10.1016/j.cofs.2020.04.006>
- Le Feunteun, S., Verkempinck, S., Flourey, J., Janssen, A., Kondjoyan, A., Marze, S., Mirade, P.-S., Pluschke, A., Sicard, J., van Aken, G., & Grauwet, T. (2021). Mathematical modelling of food hydrolysis during in vitro digestion: From single nutrient to complex foods in static and dynamic conditions. *Trends in Food Science & Technology*, 116, 870–883. <https://doi.org/10.1016/j.tifs.2021.08.030>
- Li, C., & Jin, Y. (2021). A CFD model for investigating the dynamics of liquid gastric contents in human-stomach induced by gastric motility. *Journal of Food Engineering*, 296, 110461. <https://doi.org/10.1016/j.jfoodeng.2020.110461>
- Lucas-González, R., Viuda-Martos, M., Pérez-Alvarez, J. A., & Fernández-López, J. (2018). In vitro digestion models suitable for foods: Opportunities for new fields of application and challenges. *Food Research International*, 107, 423–436. <https://doi.org/10.1016/j.foodres.2018.02.055>
- Malagelada, J.-R., Go, V. L., & Summerskill, W. (1979). Different gastric, pancreatic, and biliary responses to solid-liquid or homogenized meals. *Digestive Diseases and Sciences*, 24(2), 101–110. <https://doi.org/10.1007/BF01324736>
- Malagelada, J.-R., Longstreth, G. F., Summerskill, W. H. J., & Go, V. L. W. (1976). Measurement of gastric functions during digestion of ordinary solid meals in man. *Gastroenterology*, 70(2), 203–210. [https://doi.org/10.1016/S0016-5085\(76\)80010-8](https://doi.org/10.1016/S0016-5085(76)80010-8)
- Marciani, L., Hall, N., Pritchard, S. E., Cox, E. F., Totman, J. J., Lad, M., Hoad, C. L., Foster, T. J., Gowland, P. A., & Spiller, R. C. (2012). Preventing gastric sieving by blending a solid/water meal enhances satiation in healthy humans. *The Journal of Nutrition*, 142(7), 1253–1258. <https://doi.org/10.3945/jn.112.159830>
- Mathews, C. K., Van Holde, K. E., & Ahern, K. G. (2000). *Biochemistry* (3rd ed.). Benjamin Cummings.
- Ménard, O., Famelart, M.-H., Deglaire, A., Le Gouar, Y., Guérin, S., Malbert, C.-H., & Dupont, D. (2018). Gastric emptying and dynamic in vitro digestion of drinkable yogurts: Effect of viscosity and composition. *Nutrients*, 10(9), 1308. <https://doi.org/10.3390/nu10091308>
- Mennah-Govela, Y. A., Singh, R. P., & Bornhorst, G. M. (2019). Buffering capacity of protein-based model food systems in the context of gastric digestion [10.1039/C9FO01160A]. *Food & Function*, 10(9), 6074–6087. <https://doi.org/10.1039/C9FO01160A>
- Mudie, D. M., Murray, K., Hoad, C. L., Pritchard, S. E., Garnett, M. C., Amidon, G. L., ... Marciani, L. (2014). Quantification of gastrointestinal liquid volumes and distribution following a 240 mL dose of water in the fasted state. *Molecular Pharmacology*, 11(9), 3039–3047. <https://doi.org/10.1021/mp500210c>
- Murakami, U., & Uchida, K. (1985). Contents of myofibrillar proteins in cardiac, skeletal, and smooth muscles. *The Journal of Biochemistry*, 98(1), 187–197. <https://doi.org/10.1093/oxfordjournals.jbchem.a135257>
- Ovesen, L., Bendtsen, F., Tage-Jensen, U., Pedersen, N. T., Gram, B. R., & Rune, S. J. (1986). Intraluminal pH in the stomach, duodenum, and proximal jejunum in normal subjects and patients with exocrine pancreatic insufficiency. *Gastroenterology*, 90(4), 958–962. [https://doi.org/10.1016/0016-5085\(86\)90873-5](https://doi.org/10.1016/0016-5085(86)90873-5)
- Pal, A., Brasseur, J. G., & Abrahamsson, B. (2007). A stomach road or “Magenstrasse” for gastric emptying. *Journal of Biomechanics*, 40(6), 1202–1210. <https://doi.org/10.1016/j.jbiomech.2006.06.006>
- Pandolf, S. J. (2011). The exocrine pancreas. Colloquium series on integrated systems physiology: from molecule to function.
- Piper, D., & Fenton, B. H. (1965). pH stability and activity curves of pepsin with special reference to their clinical importance. *Gut*, 6(5), 506. <https://doi.org/10.1136/gut.6.5.506>
- Rivera del Rio, A., Keppler, J. K., Boom, R. M., & Janssen, A. E. M. (2021). Protein acidification and hydrolysis by pepsin ensure efficient trypsin-catalyzed hydrolysis. *Food & Function*, 12(10), 4570–4581. <https://doi.org/10.1039/D1FO00413A>
- Rivest, J., Bernier, J., & Pomar, C. (2000). A dynamic model of protein digestion in the small intestine of pigs. *Journal of Animal Science*, 78(2), 328–340. <https://doi.org/10.2527/2000.782328x>
- Roman, C. (1982). Nervous control of esophageal and gastric motility. In *Mediators and drugs in gastrointestinal motility I* (pp. 223–278). Springer. https://doi.org/10.1007/978-3-642-68437-1_9
- Rønnestad, I., Akiba, Y., Kaji, I., & Kaunitz, J. D. (2014). Duodenal luminal nutrient sensing. *Current Opinion in Pharmacology*, 19, 67–75. <https://doi.org/10.1016/j.coph.2014.07.010>
- Scholten, H., Kramer, M. R., van Ammers, E. W., Smolenaars, H., van Wijk, M., Weistra, J., & van Heuveln, J. (1998–2020). *Simulation and modelling assistant for research and training*. Wageningen University.
- Schop, M., Jansman, A. J. M., de Vries, S., Ellis, J. L., & Gerrits, W. J. J. (2020). Modelling digestion and absorption kinetics of nutrients in growing pigs. *Modelling digestion kinetics in pigs. Predicting nutrient absorption based on diet and ingredient properties*. <https://doi.org/10.18174/507537>
- Siegel, J., Urbain, J., Adler, L., Charkes, N., Maurer, A., Krevsky, B., Knight, L., Fisher, R., & Malmud, L. (1988). Biphasic nature of gastric emptying. *Gut*, 29(1), 85–89. <https://doi.org/10.1136/gut.29.1.85>
- Simonian, H. P., Vo, L., Doma, S., Fisher, R. S., & Parkman, H. P. (2005). Regional postprandial differences in pH within the stomach and gastroesophageal junction. *Digestive Diseases and Sciences*, 50(12), 2276–2285. <https://doi.org/10.1007/s10620-005-3048-0>
- Strathe, A. B., Danfær, A., & Chwalibog, A. (2008). A dynamic model of digestion and absorption in pigs. *Animal Feed Science and Technology*, 143(1), 328–371. <https://doi.org/10.1016/j.anifeedsci.2007.05.018>
- The UniProt Consortium. (2018). UniProt: A worldwide hub of protein knowledge. *Nucleic Acids Research*, 47(D1), D506–D515. <https://doi.org/10.1093/nar/gky1049>
- Turfus, S. C., Delgoda, R., Picking, D., & Gurley, B. J. (2017). Pharmacokinetics. In S. Badal, & R. Delgoda (Eds.), *Pharmacognosy* (pp. 495–512). Academic Press. <https://doi.org/10.1016/B978-0-12-802104-0.00025-1>
- van Aken, G. A. (2020). *In silico digestive physiology modeling*. Retrieved 04-2022 from <http://www.insightfoodinside.com/Food-interacting-with-the-body/In-silico-digestion-modelling/>.
- van der Schoor, S. R. D., Reeds, P. J., Stoll, B., Henry, J. F., Rosenberger, J. R., Burrin, D. G., & van Goudoever, J. B. (2002). The high metabolic cost of a functional gut. *Gastroenterology*, 123(6), 1931–1940. <https://doi.org/10.1053/gast.2002.37062>
- van der Sman, R. G. M., Houlder, S., Cornet, S., & Janssen, A. (2020). Physical chemistry of gastric digestion of proteins gels. *Current Research in Food Science*, 2, 45–60. <https://doi.org/10.1016/j.crf.2019.11.003>
- Vella, A. (2016). Gastrointestinal Hormones and Gut Endocrine Tumors. In S. Melmed, K. S. Polonsky, P. R. Larsen, & H. M. Kronenberg (Eds.), *Williams textbook of endocrinology* (13th ed., pp. 1701–1722). Elsevier. <https://doi.org/10.1016/B978-0-323-29738-7.00038-1>
- Versantvoort, C. H. M., & Rompelberg, C. J. M. (2004). Development and applicability of an in vitro digestion model in assessing the bioaccessibility of contaminants from food. From <https://www.rivm.nl/bibliotheek/rapporten/320102002.pdf>.
- Vertzoni, M., Dressman, J., Butler, J., Hempenstall, J., & Reppas, C. (2005). Simulation of fasting gastric conditions and its importance for the in vivo dissolution of lipophilic compounds. *European Journal of Pharmaceutical and Biopharmaceutics*, 60(3), 413–417. <https://doi.org/10.1016/j.ejpb.2005.03.002>
- Weinstein, D., Derijke, S., Chow, C., Foruraghi, L., Zhao, X., Wright, E., Whatley, M., Maass-Moreno, R., Chen, C., & Wank, S. (2013). A new method for determining gastric acid output using a wireless pH-sensing capsule. *Alimentary Pharmacology & Therapeutics*, 37(12), 1198–1209. <https://doi.org/10.1111/apt.12325>
- Worsøe, J., Fynne, L., Gregersen, T., Schlageter, V., Christensen, L. A., Dahlerup, J. F., ... Krogh, K. (2011). Gastric transit and small intestinal transit time and motility assessed by a magnet tracking system. *BMC Gastroenterology*, 11, 145. <https://doi.org/10.1186/1471-230X-11-145>
- Yu, L. X., Crison, J. R., & Amidon, G. L. (1996). Compartmental transit and dispersion model analysis of small intestinal transit flow in humans. *International Journal of Pharmaceutics*, 140(1), 111–118. [https://doi.org/10.1016/0378-5173\(96\)04592-9](https://doi.org/10.1016/0378-5173(96)04592-9)